

A-28 APPLICATION OF ELECTRON FRACTOGRAPHY  
AND FRACTURE MECHANICS TO FATIGUE CRACK PROPAGATION

Richard W. Hertzberg<sup>1</sup>  
Paul C. Paris<sup>2</sup>

Abstract

Fatigue crack propagation in an aluminum alloy is examined using electron fractography and analytical methods of fracture mechanics. It is observed that the stress-intensity-factor correlates fatigue crack growth rates determined both by measurements taken during a fatigue test and/or measurements of the fatigue striations found on the fracture surface. The latter correlation is considered to be of importance for post fracture analysis of engineering service failures.

A plane strain to plane stress fracture mode transition is observed where the macroscopic fracture plane switches from one normal to the applied load to one inclined approximately 45 degrees to the applied load and the sheet thickness. The transition is found to be related to the stress-intensity-factor and its effect on the plastic zone size ahead of the crack tip. A constant plastic zone size to sheet thickness ratio is observed for the transition point in the three sheet thicknesses investigated. A difference between the fracture mechanisms associated with plane strain and plane stress fatigue crack propagation is noted due to the absence of striations during plane stress crack propagation.

Introduction

In recent years, many investigators have examined the significant loading parameters associated with fatigue crack propagation in alloy sheet materials by monitoring crack growth rates<sup>1-10</sup>. While some studies have been empirical in nature, others have considered models based upon fracture criteria and dimensional analysis<sup>2,4</sup>. The validity and general applicability of all existing parametric relations between stress environment and fatigue crack propagation was the subject of earlier work<sup>6</sup>. It was found that the fracture mechanics approach gave the most consistent agreement with the experimental data.

---

1 Assistant Professor of Metallurgy, Lehigh University, Bethlehem, Pennsylvania.

2 Prof. of Mechanics, Lehigh University, Bethlehem, Pennsylvania.

In a quite different approach to the problem, many investigators<sup>11-23</sup> have examined the resulting fracture surfaces for possible clues as to the nature of fatigue crack propagation. In a sense, this type of study has been concerned with obtaining information "after the fact". Pioneering work by Crussard and co-workers<sup>11,12</sup> revealed that many areas of the fracture surface of specimens broken in fatigue contained countless thousands of parallel markings called striations. Subsequently, much effort has been devoted to the study of the relationship between these striations and fatigue crack growth<sup>16,20,24,25</sup>.

It is the purpose of the current work to employ the techniques of "post fracture" electron fractography in direct combination with "in progress" crack propagation observations to further explore the subject of fatigue crack propagation. The basic objectives will, therefore, be to generate sufficient data to critically evaluate the usefulness of the stress intensity parameter for correlation of fatigue crack growth rate data<sup>26</sup>, to determine whether this same parameter can correlate fatigue striation data and, hence, establish a relationship between "in progress" and "post fracture" data. Moreover, an attempt will be made to describe macroscopic and microscopic changes in the fracture surface appearance and its relationship to a measure of the crack tip stress field conditions, i.e., the stress-intensity-factor.

#### Some Elements of Fracture Mechanics

Based upon the method of Westergaard<sup>27</sup>, Irwin<sup>28</sup> extensively developed those concepts of fracture mechanics which deal with the elastic stress conditions near the tip of a sharp crack in a plate. It was found possible to define these stress fields by the following equations:

$$\sigma_y = \frac{K}{\sqrt{2r}} \cos \frac{\theta}{2} \left[ 1 + \sin \frac{\theta}{2} \sin \frac{3\theta}{2} \right]$$

$$\sigma_x = \frac{K}{\sqrt{2r}} \cos \frac{\theta}{2} \left[ 1 - \sin \frac{\theta}{2} \sin \frac{3\theta}{2} \right]$$

$$\tau_{xy} = \frac{K}{\sqrt{2r}} \sin \frac{\theta}{2} \cos \frac{\theta}{2} \cos \frac{3\theta}{2}$$

$$\tau_{yz} = \tau_{xz} = 0$$

Furthermore, for conditions of plane stress

$$\sigma_z = 0$$

while for plane strain

$$\sigma_z = \nu (\sigma_x + \sigma_y)$$

$\sigma_x, \sigma_y, \sigma_z, \theta$  and  $r$  are diagrammatically shown in Figure 1 and  $\nu$  is Poisson's ratio.  $K$  is defined as the stress-intensity-factor and is related to the applied load and a function of the crack length which depends upon the specimen configuration and the type of loading<sup>28</sup>.

It is important to note that in any material capable of plastic flow, a small region of plasticity will exist at the tip of a crack as a result of the exceedingly high localized stresses. By inserting the elastic stress distribution associated with the crack (as given above) into a yield criteria, it is easy to show that the size of the plastic zone,  $r_y$ , is related to the stress intensity factor and the material's yield strength, so that

$$r_y = \frac{K^2}{2\sigma_y^2}$$

#### Macroscopic Fracture Mode Transition

In conducting tensile fracture tests of engineering sheet materials, it was observed by many that the gross plane of fracture was either sometimes approximately normal to the direction of applied load, sometimes inclined at an angle of about 45 degrees to the loading direction and sheet thickness or most often a combination of both normal and inclined to the loading direction<sup>29</sup>. Similar observations have been made in the course of fatigue crack propagation studies<sup>3,30,31</sup>. Using the stress-intensity-factor, Irwin<sup>33</sup> suggested an interpretation of this fracture mode (plane) transition in terms of the size of the plastic region ahead of a crack in the sheet. He showed that, for static load conditions, when the plastic zone size was small relative to the sheet thickness, the crack progressed along a plane normal to the loading direction<sup>32</sup>. For a small plastic zone, a tensile stress perpendicular to the sheet,  $\sigma_z$ , is zero at the sheet surface but approaches  $\nu(\sigma_x + \sigma_y)$  in the interior due to the restriction of strain in the sheet thickness direction. Consequently, Irwin interpreted fracture along a plane normal to the loading direction as evidence of plane strain crack propagation. When the plastic zone size is large compared to the sheet thickness, the fracture path shifts to planes oriented approximately 45 degrees to the loading direction and through the thickness direction. For the large plastic zone, the stress in the thickness direction is approximately zero across the entire sheet thickness offering no restriction to strain in that direction. Fracture along these inclined planes was observed by Irwin in conjunction with plane

stress crack propagation. Such reasoning led him to conclude that the fracture mode transition from flat to shear failure would occur when the plastic zone size became a sufficiently large fraction of the sheet thickness. Experimental results did, in fact, show that for conditions of static loading, a fracture mode transition from flat to shear failure is observed in a range of essentially constant plastic zone size to sheet thickness ratio<sup>29</sup>.

#### Application of Fracture Mechanics to Fatigue Crack Propagation

It has been reasoned that if stress-intensity-factors could be used to evaluate the fracture toughness characteristics of high strength materials for conditions of static loading<sup>29</sup>, they might equally be applied to the problem of moving cracks during cyclic loading<sup>7</sup>. In an attempt to synthesize fatigue crack propagation in terms of one major variable, the stress-intensity range,  $\Delta K$  (i.e.,  $K_{\max} - K_{\min}$ ) was considered<sup>7</sup>. The companion parameter describing the ratio of mean load to load range  $\frac{K_{\text{mean}}}{\Delta K}$  (defined as  $\gamma$ ) was found to be of secondary importance. Using  $\Delta K$ , strong correlation was obtained for fatigue crack growth in several steel and aluminum alloys as well as for titanium and magnesium<sup>7</sup>. It was, therefore, concluded that since a correlation was obtained for FCC, BCC and HCP metals, the stress-intensity-factor has been shown to be a most appropriate loading parameter associated with fatigue crack propagation.

#### Correlation of $K$ and Crack Growth Rate

Figures 2, 3, and 4 reveal the test data from this investigation for 2024-T3 aluminum sheet with thicknesses of .064, .094, and .126 inches and shows the correlation over four orders of magnitude of crack growth rates. The data for growth rates above  $10^{-5}$  inches per cycle were obtained from single edge notch specimens tested on an Instron machine at a cycle frequency of 30-45 cpm. Growth rate data below  $10^{-5}$  inches per cycle were obtained from central notch specimens tested on an Amsler Vibrophore machine at a cycle frequency of 5000-8000 cpm. The results illustrate that the stress-intensity-factor range,  $\Delta K$ , provides strong correlation between the stress conditions at the tip of the propagating crack and the resulting crack growth rate.

It is to be noted that the growth rate measurements plotted for the centrally notched specimens were for one crack rather than the total growth of both cracks. This was done to make a direct comparison with the growth rate data from single edge-notched specimens. Since both crack tips in the centrally notched specimen experience the same stress-intensity conditions, one would expect similar crack growth rates. It was found that this is not always the case. Several specimens exhibited

the peculiar behavior wherein one crack first grew at a slower rate than expected on the basis of the stress-intensity conditions and then subsequently propagated at a rate somewhat faster than anticipated. Further, it was noted that one crack tip very often counter-balanced the behavior of its companion crack tip by propagating rapidly when the latter moved slowly and then slowing down when the latter accelerated. Consequently, the overall average crack growth rate tended to remain constant. A typical example of this behavior is illustrated in Figure 5 where crack length versus number of cycles is plotted for companion crack tips of one specimen.

The explanation for this behavior is at present unclear. Load eccentricity caused by a subtle shift in the loading grips may cause a change in the relative growth rates of the two cracks. It is also possible that local microstructural changes such as grain orientation may cause discontinuous changes in the growth rate at the tip of each crack.

#### Macroscopic Fracture Mode Transition

As anticipated, a fracture mode transition from flat to shear failure was observed in all specimens during the latter stages of testing, where the stress-intensity-factor was largest due to the large crack size. In all cases, the flat portion of the crack was gradually eliminated by the increasing width of the shear lips till full shear was developed. The calculated values of stress-intensity at transition (based upon the maximum applied stress and the maximum length of the flat portion of the crack) increased with increasing thickness of the test panel (Table I) as had been previously observed for the case of static tensile tests. Furthermore, calculations based on the plastic zone size to sheet thickness ratio at the point where flat fracture was completely eliminated revealed a constant ratio for the three thicknesses of 2024-T3 aluminum alloy. Figure 6 and Table I shows this ratio to be a value of approximately 0.5.

#### General Microscopic Appearance of Fatigue Fracture Surfaces

The macroscopically flat portion of the fracture surface produced under plane strain conditions was composed of three different morphological appearances: areas which contained well-defined fatigue striations (Figure 7), areas which contained ill-defined striations (Figure 8), and areas which consisted of a rumpled appearance with no evidence of fatigue striations (Figure 9). (The fractographs shown in Figure 7, 8 and 9 were all taken from the same replica.) Areas devoid of striations have also been observed by others in the field of electron fractography<sup>30,31</sup>. Unfortunately, many of the published works on the fractographic examination of fatigue fracture surfaces make re-

ference only to the form and size of the striations and lead the inexperienced reader to the tacit conclusion that fatigue fracture surfaces consist only of these striations; this is definitely not the case.

The plane stress shear fracture surface revealed a considerably different morphology. As the flat region gradually shifted to the shear plane at 45 degrees to the tensile axis, fewer striated regions were observed on the fracture surface. During later stages of crack propagation in the full shear mode, no striations were present at all. Associated with the decreasing incidence of striations as the shear wall fully developed were an increasing number of examples of ductile rupture. "Elongated dimples" with the long axis perpendicular to the direction of crack propagation were found in increasing numbers as the 45° through the sheet shear plane fracture surface developed (Figure 10).

#### Correlation Between $\Delta K$ and Striation Spacings

Figures 2, 3, 4 and 11 reveal the excellent correlation between stress-intensity values and measurements of the striation spacings found on the fracture surface. It is felt that the relatively small degree of scatter was due to the fact that at least ten and as many as twenty measurements were taken of the striation spacings within a total crack growth increment of less than .06 inches. The data plotted were the average value of these measurements. It should be noted, therefore, that the data shown in Figures 2, 3, 4 and 11 represent 1200 to 1500 separate measurements of striation spacings taken from the fracture surfaces.

It was found that the maximum striation spacings were often two and sometimes three times larger than the minimum spacings recorded. Because of these local variations in the crack growth rate, it is felt that a few isolated measurements of striation spacings are insufficient to describe the mean growth rate of the crack in a specific macroscopic region of the fracture surface. This fact may have been partially responsible for the difference in results observed by Pelloux<sup>24</sup> and Schijve<sup>25</sup>.

The range of data over which fatigue striations were observed was from approximately  $10^{-6}$  to  $10^{-4}$  inches per striation spacing. The limit as to the maximum size of the striations was set by the incidence of plane stress crack propagation along 45 degree fracture planes. The smallest recorded striation spacing was  $7 \times 10^{-7}$  inches wide or about 175Å (Figure 12) (the smallest striation recorded in the literature by Christensen<sup>33</sup> was 200Å). It is not clear whether this value represents a minimum spacing below which striations will not form. Considering striation formation to be caused by some dislocation process, it would be expected that a minimum striation spacing should exist in

the order of some multiple of the dislocation burger's vector. The precise value of this lower limit was not found in this investigation because of the limiting resolving power of the techniques employed in the fractographic examination.

#### Discussion

The correlation between the range of the stress-intensity-parameter,  $\Delta K$ , with fatigue crack growth rates and striation spacings for the three sheet thicknesses investigated offers further evidence that the stress-intensity-factor is a powerful unifying parameter for studies involving the effect of the crack tip stress field on fatigue crack propagation. From the data shown in Figures 2, 3 and 4, it is observed that a one-to-one relationship exists between crack growth rates and striation spacings in the range of  $1-4 \times 10^{-5}$  inches per cycle. However, the striations were found to be larger for growth rates below  $10^{-5}$  inches/cycle but somewhat smaller than the overall growth rates above  $5 \times 10^{-5}$  inches/cycle. This variation in behavior illustrates the danger involved in making gross generalizations on fracture surface appearance based upon a limited selection of data.

Since all of the tests were conducted at approximately the same ratio of  $K$  mean to  $\Delta K$ , it was not possible to evaluate the importance of the relative mean load,  $\gamma$ . Earlier work has found this parameter to be of second order importance compared to  $\Delta K$  for correlation of fatigue data<sup>6</sup>.

The experimental data showed a second order dependence upon the frequency of loading. It is seen that the data obtained at the higher frequencies of loading (5000 to 8000 cycles per minute) is shifted toward lower growth rates for a given value of stress-intensity. This effect has been previously reported in the literature by Donaldson<sup>8</sup>, and Anderson<sup>10</sup>, who found the frequency effect to be of secondary importance compared to the stress-intensity-factor range,  $\Delta K$ . The nature of this frequency dependence is not clear although it has been tentatively associated with a strain rate dependence and/or to an argument based on metallurgical instabilities resulting from deformation induced heat generation at the crack tip.

As shown in Figure 6, the fracture mode transition from plane strain to plane stress crack propagation observed in the fatigue tests was related to the stress-intensity-factor by means of the plastic zone size. In addition, the position of this transition on the fracture surface was quantitatively determined by the computed relative plastic zone size to sheet thickness ratio. One may conclude that the importance of the stress-intensity-factor as a means of correlating fatigue crack propagation data is further enhanced by its ability to also describe the nature of the fracture mode transition.

The horizontal bars in Figures 2, 3 and 4 represent the stress-intensity-factor values for each single-edge notched specimen at the point of fracture mode transition. It is important to note that there is no discontinuity in the value or slope of any of these curves that can be associated with the fracture mode transition. This observation is contrary to Liu's<sup>2</sup> thought that stress-intensity and crack growth data might be related by two different power functions and that the transition from one to the other occurred at the point of fracture mode transition.

From the fractographic results, it is clear that there exists a difference between plane strain and plane stress fracture mechanisms. By considering the conditions associated with plane strain and plane stress crack growth, one may understand why striations would be expected to form during plane strain propagation but would be expected to be absent during plane stress propagation.

For conditions of plane strain, the amount of plastic flow is small while  $\sigma_z$ , the stress perpendicular to the sheet, is large. For this case, it has been shown that the planes of maximum shear stress ahead of a crack tip are perpendicular to the sheet and inclined  $\pm 60$  to 70 degrees to the plane of the crack<sup>34</sup>. Consequently, when plane strain conditions are met, slip will occur on these two maximum shear planes (Figure 13a). The exact angle between the maximum shear planes and the plane of the crack is expected to depend upon prior amounts of plastic deformation but the shear planes are always perpendicular to the sheet. While the general plane of the crack is normal to the applied loading for conditions of plane strain, fatigue damage occurs along the shear planes inclined to the plane of the crack. Consequently, it would be possible to form striations on the fracture surface since striations can be generally thought of as having been produced by some mechanism producing slip motion in and out of the plane of the crack so as to produce fracture surface markings parallel to the advancing crack front.

For conditions of plane stress, the situation is markedly different since the amount of plastic flow at the crack tip is much larger while  $\sigma_z$  is approximately equal to zero. For this case, the planes of maximum shear are oriented at approximately 45 degrees to both the plane of the crack and the plane of the sheet. When slip occurs, it will be along these shear planes and in a direction from one surface of the sheet to the other; the slip direction is, therefore, parallel to the leading edge of the advancing crack front (Figure 13b). For this stress condition, it is not possible to describe the formation of striations which may be considered to be essentially surface undulations. The inability to form striations is due to the absence of a slip process that can move in and out of the plane stress shear planes (oriented through the sheet thickness at 45 degrees) and produce fracture surface markings parallel to the advancing crack front.

The flat to shear mode transition and the associated elimination of fatigue striations was not an abrupt one. As noted in Figures 2, 3 and 4, there were data recorded for the striation spacings at stress intensity levels above those associated with the fracture mode transition. Since the fracture mode transition was a gradual process, one would expect there to be isolated flat regions where striations would be observed on the shear wall. These flat regions decreased in number as the shear wall became steeper until finally no striations were observed at the large values of stress intensity. In place of the striations an increasing number of "elongated dimples" appeared, oriented with the long axis perpendicular to the crack growth direction. The orientation of these "dimples" was consistent with both the direction of shear along the shear walls associated with plane stress conditions and the shearing direction responsible for the formation of the "dimples". As proof of the competing processes of striation formation on the isolated flat portions of the fracture surface and the "elongated dimples" along the shear walls, Figure 14 reveals the presence of both striations (A) and "elongated dimples" (B) in adjacent regions. Note that while there was a stress component parallel to the "dimples" to form them along the shear wall, there must also have been a perpendicular component of stress so as to form the striations within the flat regions.

It is possible to conclude that plane strain and plane stress fatigue crack propagation mechanisms are most certainly different from one another. It is worth further note that an important implication arises from this conclusion. Since no striations are to be found during plane stress crack propagation (i.e., high stress intensity conditions) it is difficult, if not impossible, to differentiate fractographically between high rate fatigue failures conducted under plane stress conditions and shear type tensile failures; both fracture surfaces would reveal "elongated dimples" oriented in the same direction. This poses an obvious problem in post fracture analysis with respect to the above situation unless one is able to find isolated evidence of striations produced in some localized flat portions of the fracture surface.

### Conclusions

Based upon the experimental results and subsequent discussion, the following conclusions may be drawn:

1. Fatigue crack growth rates measured with a traveling microscope were related to the stress-intensity conditions at the crack tip and were not dependent upon sheet thickness (i.e., dependent in a very secondary manner, if at all).
2. The frequency of loading was of minimal importance in the correlation of crack growth rates with the stress-intensity-factor.

3. The fracture mode transition from flat to shear type failure (i.e., plane stress vs. plane strain) was related to the stress-intensity conditions at the crack tip.

4. The stress-intensity-factor at the fracture mode transition point increased with increasing sheet thickness while a constant plastic zone size to sheet thickness ratio described the transition behavior in all sheets.

5. Fatigue striations were readily observed within the plane strain fracture region but were absent from plane stress fracture surface. This can be and was discussed in terms of the favorable slip modes associated with plane strain and plane stress crack propagation.

6. Fatigue crack growth rates measured from fatigue striation spacings were correlated with the stress-intensity conditions at the crack tip and were independent of sheet thickness.

#### Acknowledgement

The support of the National Aeronautics and Space Agency for this research under Grant Nsg 410 is gratefully acknowledged.

#### References

1. Head, A.K., "The Growth of Fatigue Cracks", Phil Mag, Vol. 44, Series 7, (1953), p.925.
2. Liu, H.W., "Fatigue Crack Propagation and the Stresses and Strains in the Vicinity of a Crack", Applied Material Research, Vol. 3, No. 4, (1964), p.229.
3. Weibull, W., "A Theory of Fatigue Crack Propagation in Sheet Specimens", Acta Met, Vol. 11, No. 7, (1963), p.725.
4. Frost, N.E. and Dugdale, D.S., "The Propagation of Fatigue Cracks in Sheet Specimens", Journal of the Mechanics and Physics of Solids, Vol. 6, No. 2, (1958), p.92.
5. McEvily, A.J. and Illg, W. "The Rate of Crack Propagation in Two Aluminum Alloys", NACA Technical Note 4394, September 1958.
6. Paris, P. and Erdogan, F., "A Critical Analysis of Crack Propagation Laws", J. Basic Eng., Trans. ASME, Series D, Vol. 85, No.4, (1963), p. 528.

7. Paris, P., "The Growth of Cracks Due to Variations in Load", h.D. Dissertation, Lehigh University, September 1962
8. Donaldson, D.R. and Anderson, W.E., "Crack Propagation Behavior of Some Airframe Materials", Proc. of the Crack Propagation Symposium, Cranfield, England, (1961), p. 375.
9. Paris, P., Gomez, M.P. and Anderson, W.E., "A Rational Analytic Theory of Fatigue", The Trend in Engineering, Vol. 13, (January 1961), p. 9.
10. Anderson, W.E. and Paris, P., "Evaluation of Aircraft Material by Fracture", Metals Engineering Quarterly, ASM, Vol. 1, No.2, (May 1961).
11. Crussard, C., Borione, R. Plateau, J., Morillon, Y. and Maratray, F., "A Study of Impact Tests and the Mechanism of Brittle Fracture", Journal of the Iron and Steel Institute, Vol. 183, (1956), p.146.
12. Crussard, C. Plateau, J. Tamhanker, R. and Lajeunesse, D. "A Comparison of Ductile and Fatigue Fractures" Fracture, New York Technology Press, M.I.T. and John Wiley, (1959), p. 524.
13. Pelloux, R.M.N., "The Analysis of Fracture Surfaces by Electron Microscopy", Boeing Scientific Research Laboratories, Report DI-82-0169-RI, December 1963.
14. Forsyth, P.J.E. and Ryder, D.A., "Some Results of the Examination of Aluminum Alloy Specimen Surfaces", Metallurgia, Vol. 63, (1961), p. 117.
15. Stubbington, C.A., "Some Observations on Air and Corrosion Fatigue of an Aluminum-7.5% Zinc-2.5% Magnesium Alloy", Metallurgia, Vol. 68, (1963), p.109.
16. Forsyth, P.J.E. and Ryler, D.A., "Fatigue Fracture", Aircraft Engineering, Vol. 32, No.374, (1960), p.96.
17. Beachem, C.D., "Electron Fractographic Studies of Mechanical Fracture Processes in Metals", Trans. ASME, Journal of Basic Engineering, 1964.
18. Beachem, C.D. and Pelloux, R.M.N., "Electron Fractography -- A Tool for the Study of Micro Mechanisms of Fracturing Processes", presented at Sixty-seventh Annual Meeting of ASTM, Chicago, June 1964.

19. Warke, W.R. and McCall, J.L., "Using Electron Microscopy to Study Metal Fracture", Society of Automotive Engineers, Paper No.828D, April 1964.
20. Piper, D.E., Quist, W.E. and Anderson, W.E., "The Effect of Composition on the Fracture Properties of 7178-T6 Aluminum Alloy Sheet", presented at AIME Fall Meeting, Philadelphia, October 1964.
21. Carmen, C. and Shuler, M., "Low Cycle Fatigue Properties of 18 Ni-Co-Mo 250 Maraging Steel", presented at ASTM Subcommittee on Electron Fractography, Schenectady, New York, September 1964.
22. Laird, C. and Smith, G.C., "Crack Propagation in High Stress Fatigue", Phil. Mag., Vol. 7, (1962), p. 847.
23. McEvily, Jr., A.J., Boettner, R. C. and Johnston, T.L., "On the Formation and Growth of Fatigue Cracks in Polymers", presented at Tenth Sagamore Army Materials Research Conference, August 1963.
24. Pelloux, R.M.N., "Fractographic Analysis of the Influence of Constituent Particles on Fatigue Crack Propagation in Aluminum Alloys", Trans. ASM, Vol. 57, No.2, (1964), p.511.
25. Schijve, J., "Analysis of the Fatigue Phenomenon in Aluminum Alloys", Holland, July 1964.
26. Paris, P., "The Mechanics of Fracture Propagation and Solutions to Crack Arrestor Problems", Boeing Company, Doc. No. D2-2195, September 1957.
27. Westergaard, H.M., "Bearing Pressures and Cracks", Journal of Applied Mechanics, ASME, June 1939.
28. Irwin, G.R., "Fracture", Handbuch der Physik, Vol.VI, Springer, (1958), pp. 551-590.
29. First Report of a Special ASTM Committee on Fracture Testing of High Strength Materials, ASTM Bulletin, January 1960.
30. McMillan, C., Private Communication.
31. Beachem, C.D., Private Communication.
32. Irwin, G.R., "Fracture Mode Transition for a Crack Traversing a Plate", Trans. ASME, Vol. 82, Series D, No.2, (1960), p.417.
33. Christensen, R.H., "Cracking and Fracture in Metals and Structures", Proc. of the Crack Propagation Symposium, Cranfield, England, (1961), p.326.

34. Williams, M.L., "On the Stress Distribution at the Base of a Stationary Crack", Journal of Applied Mechanics, ASME, Vol. 24, (1957), p.109.

Fracture Mode Transition Data

TABLE I

Specimen #	$l^*$	$\sigma_{max}$	$K_{max}$	$r_y$	t	$r_y/t$
3A6	1.1	5320	$1.09 \times 10^4$	.0296	.064	0.46
3A8	1.09	5210	$1.06 \times 10^4$	.0279	.064	0.44
2A6	1.3	5630	$1.50 \times 10^4$	.0551	.094	0.57
2A8	1.31	4980	$1.34 \times 10^4$	.0443	.094	0.47
1G6	1.38	5630	$1.67 \times 10^4$	.0691	.126	0.55
1G8	1.33	5560	$1.54 \times 10^4$	.0585	.126	0.46
1G10	1.37	5480	$1.59 \times 10^4$	.0622	.126	0.49

- $l^*$  = crack length at point of fracture mode transition  
 $\sigma_{max}$  = maximum applied stress  
 $K_{max} = \sigma_{max} \sqrt{l} k(a/b)$   
 $r_y = \text{plastic zone size} = 1/2 \left( \frac{K_{max}}{\sigma_{ys}} \right)^2$   
 $\sigma_{ys} = 45,000 \text{ psi (2024-T3 aluminum alloy)}$

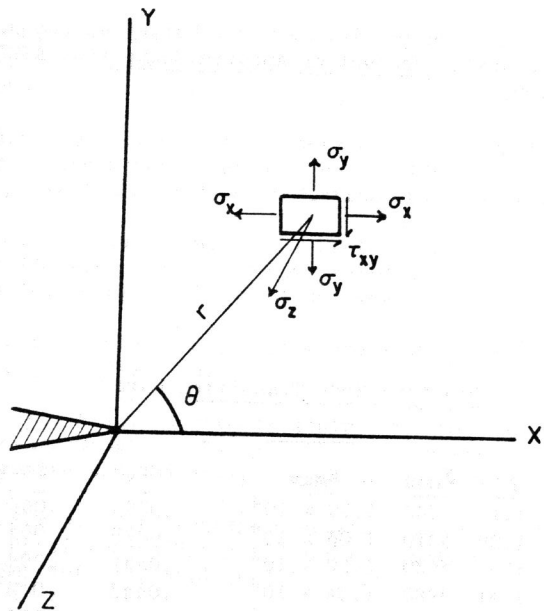


Figure 1 - Schematic Diagram Showing Stress Components in Vicinity of Crack Tip.

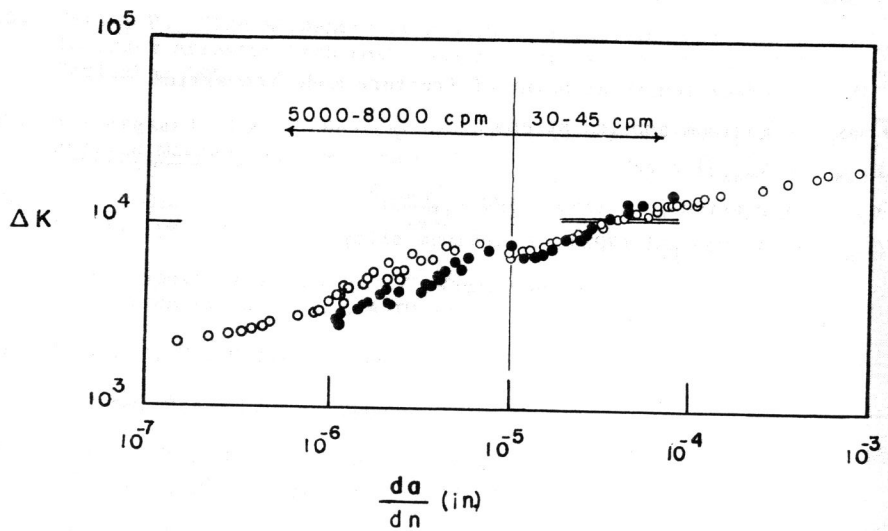


Figure 2 - Plot of Stress Intensity Range Versus Rate of Crack Propagation and Striation Spacings for .064 Gage 2024-T3 Aluminum Alloy (○ Optical Growth Rate, ● Striation Spacings).

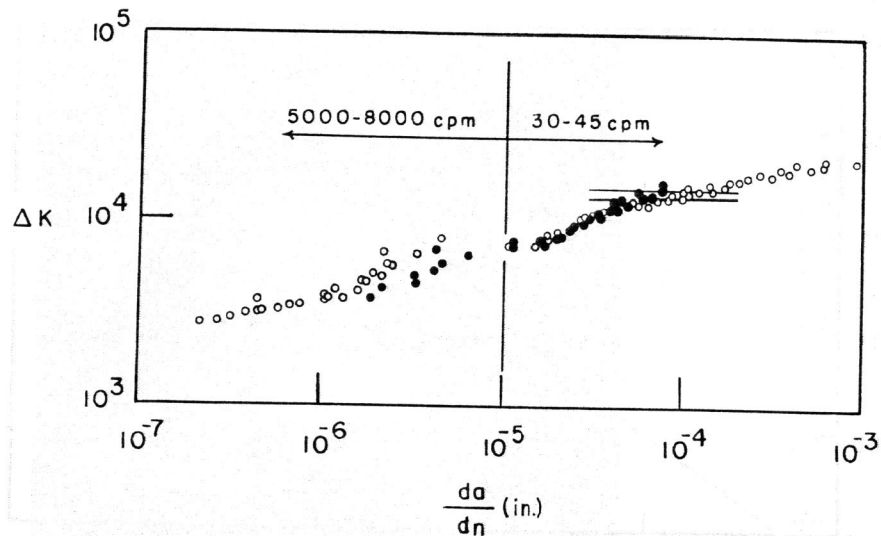


Figure 3 - Plot of Stress Intensity Range Versus Rate of Crack Propagation and Striation Spacings for .094 Gage 2024-T3 Aluminum Alloy (○ Optical Growth Rate, ● Striation Spacings).

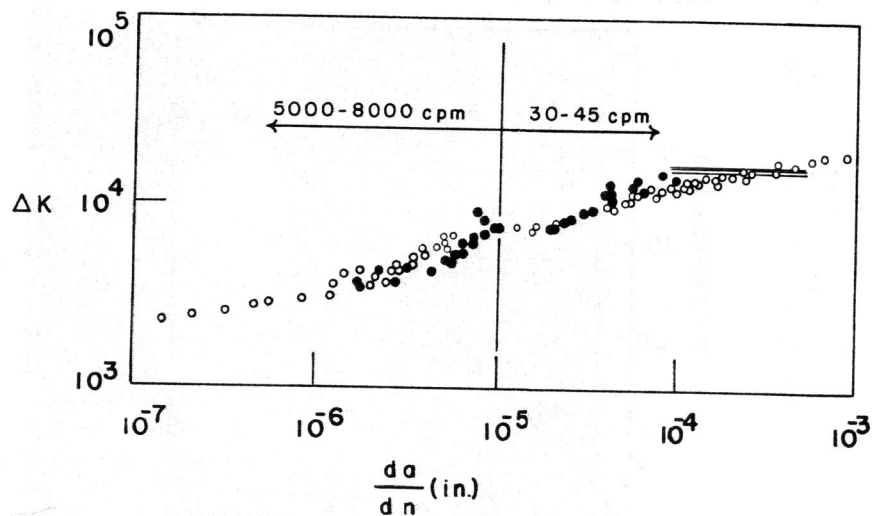


Figure 4 - Plot of Stress Intensity Range Versus Rate of Crack Propagation and Striation Spacings for .126 Gage 2024-T3 Aluminum Alloy (○ Optical Growth Rate, ● Striation Spacings).



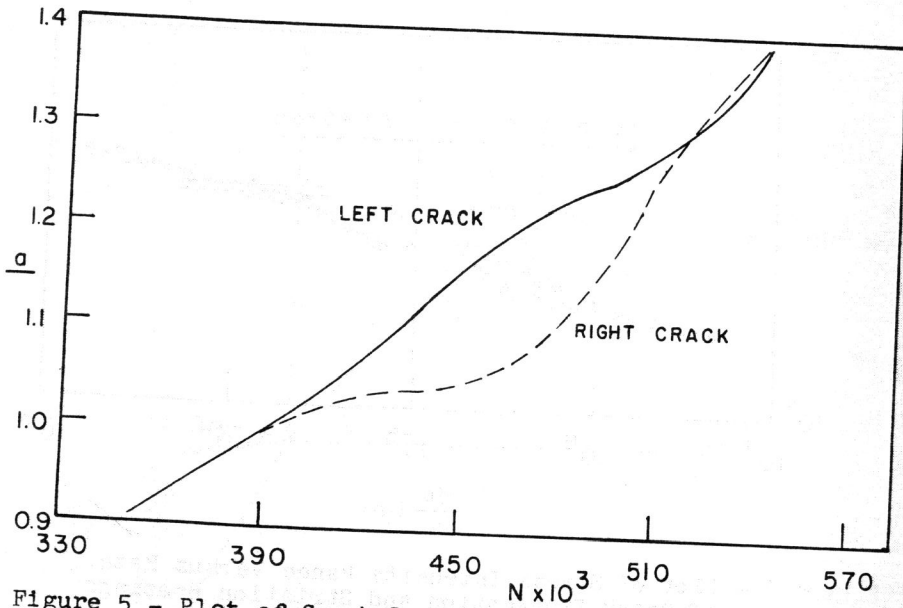


Figure 5 - Plot of Crack Length Versus Number of Loading cycles for Centrally Notched Specimen. Note Peculiar Relationship Between Growth Rates of Each Half of Crack.

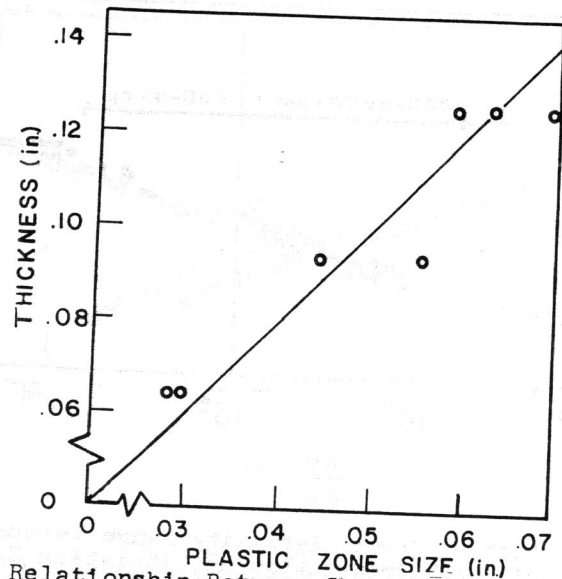


Figure 6 - Relationship Between Sheet Thickness and Crack Tip Plastic Zone Size at Point of Fracture Mode Transition.

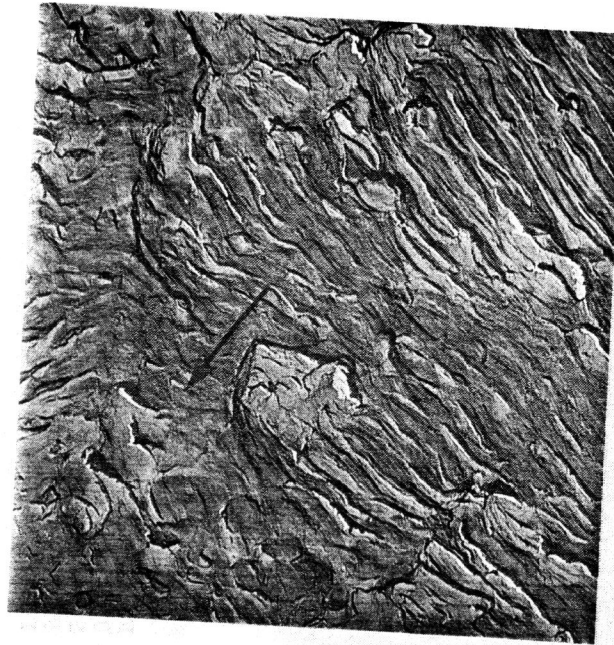


Figure 8 - Fractograph of 2024-T3 Showing Ill-Defined Fatigue Striations. Magnification: 7700X



Figure 7 - Fractograph of 2024-T3 Showing Well-Defined Fatigue Striations. Arrow Indicates Fracture Direction. Magnification: 7700X

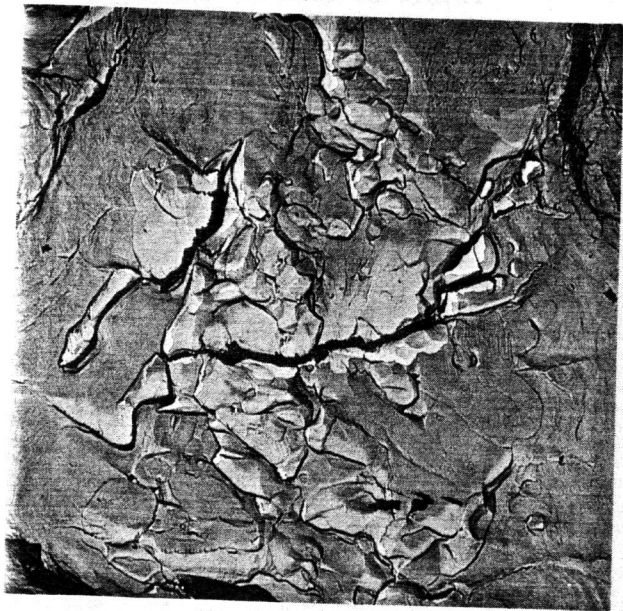


Figure 9 -  
Fractograph of 2024-T3 Showing Absence of Fatigue Striations. Magnification: 7700X



Figure 10 -  
Fractograph of 2024-T3 Showing "Elongated Dimple" Formation on Plane Stress Fracture Surface. Crack Propagation Direction Is From Lower Right to Upper Left Corner of Photograph. Magnification: 7500X

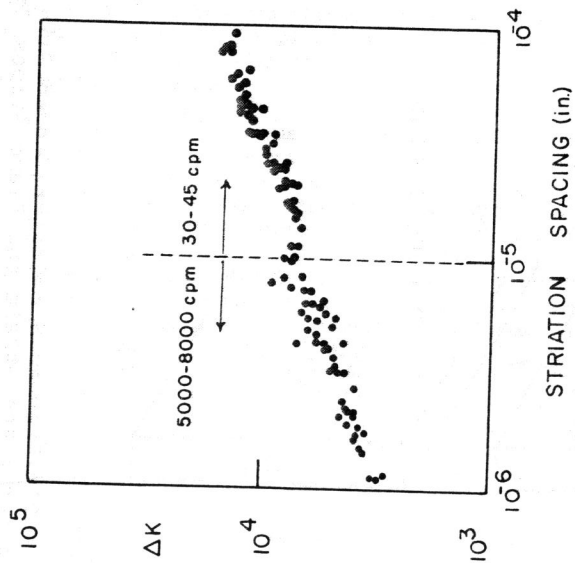


Figure 11 -  
Plot of Striation Spacings Versus Range of Stress Intensity Factor for .064, .094 and .126 Gage 2024-T3

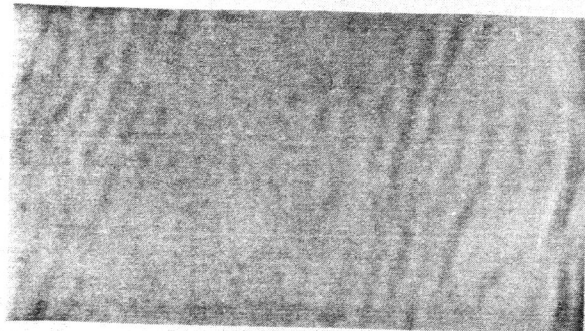


Figure 12 -  
Fractograph Showing Striations with Spacings of 175 A. Magnification: 190,000X

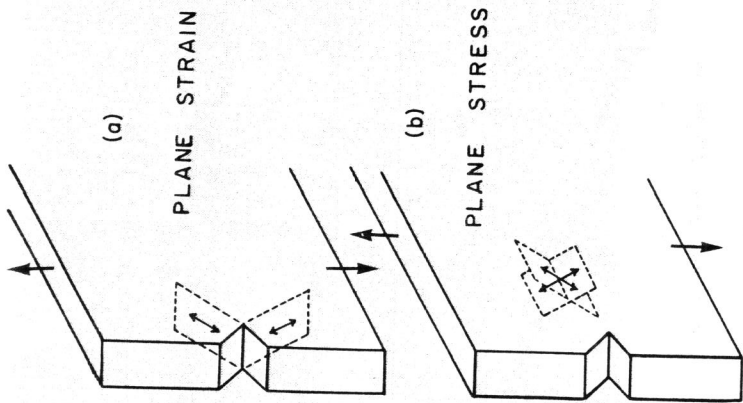


Figure 13 -

Schematic Diagram Showing Preferred Slip Mode for Plane Strain and Plane Stress Crack Propagation



Figure 14 -

Fractograph of 2024-T3 Showing Poorly Defined Fatigue Striations (A) Parallel to "Elongated Dimples" (B) Indicating Locally Competing Fracture Processes. Magnification: 7300X